Thrombospondin-1 suppresses spontaneous tumor growth and inhibits activation of matrix metalloproteinase-9 and mobilization of vascular endothelial growth factor

Juan Carlos Rodríguez-Manzaneque*, Timothy F. Lane†, María Asunción Ortega*, Richard O. Hynes‡, Jack Lawler§, and M. Luisa Iruela-Arispe*¶

*Department of Molecular, Cell, and Developmental Biology and Molecular Biology Institute, University of California, Los Angeles, CA 90095-1570; †Jonsson Comprehensive Cancer Center, Department of Obstretics and Gynecology, University of California, Los Angeles, CA 90095; ‡Howard Hughes Medical Institute, Center for Cancer Research and Department of Biology, Massachusetts Institute of Technology, Cambridge, MA 02139; and §Department of Pathology, Harvard Medical School and Beth Israel Deaconess Medical Center, Boston, MA 02215

Contributed by Richard O. Hynes, August 30, 2001

Growth of tumors and metastasis are processes known to require neovascularization. To ascertain the participation of the endogenous angiogenic inhibitor thrombospondin-1 (TSP1) in tumor progression, we generated mammary tumor-prone mice that either lack, or specifically overexpress, TSP1 in the mammary gland. Tumor burden and vasculature were significantly increased in TSP1-deficient animals, and capillaries within the tumor appeared distended and sinusoidal. In contrast, TSP1 overexpressors showed delayed tumor growth or lacked frank tumor development (20% of animals); tumor capillaries showed reduced diameter and were less frequent. Interestingly, absence of TSP1 resulted in increased association of vascular endothelial growth factor (VEGF) with its receptor VEGFR2 and higher levels of active matrix metalloproteinase-9 (MMP9), a molecule previously shown to facilitate both angiogenesis and tumor invasion. *In vitro*, enzymatic activation of proMMP9 was suppressed by TSP1. Together these results argue for a protective role of endogenous inhibitors of angiogenesis in tumor growth and implicate TSP1 in the *in vivo* regulation of metalloproteinase-9 activation and VEGF signaling.

Cancer is a multistep process that includes deregulation of cell cycle, transformation, invasion of stroma, and metastasis (1). In addition, successful establishment of solid tumors depends on neovascularization (2, 3). More recently, the contribution of angiogenesis has been further supported by the demonstration that angiogenic inhibitors suppress tumor growth. Our present understanding of the mechanism of action of most angiogenic inhibitors is limited, and further efforts are required to evaluate their effects *in vivo*.

Thrombospondin-1 (TSP1) was the first protein to be recognized as a potential endogenous suppressor of capillary morphogenesis *in vivo* (4). Most likely, modulation of vasculature is not its only function; this was well illustrated by the fact that mice lacking TSP1 developed epithelial lung hyperplasia and pneumonia with multifocal inflammatory sites, but no significant vascular phenotype was observed (5). Inflammation and several pathological conditions have been shown to induce rapid and robust TSP1 expression (6, 7). Its role in these situations remains elusive; however, it has been shown that wound healing is aberrant in TSP1-null mice (8). With respect to antiangiogenic capabilities, TSP1 inhibits endothelial cell proliferation (9) and migration (10) and can induce endothelial apoptosis (11, 12). In addition, xenograft implants of tumor cells transfected with TSP1 developed smaller tumors than the parental cell lines in a variety of assays (13–16), and fusion proteins and peptides from specific domains of TSP1 have been shown to inhibit proliferation of melanoma cells and reduce tumor growth in immunosuppressed animals (17). In clinical studies, expression of TSP1 has been inversely correlated with malignant progression of breast cancer, melanoma, and lung carcinomas (18, 19). A hypothesis consistent with these data is that TSP1 inhibits tumor growth by an antiangiogenic mechanism. However, these previous studies did not test the influence of TSP1 on spontaneous tumor progression. To address this question directly, we used a genetic approach to study mammary tumor development in immunocompetent mice with engineered variations of TSP1 production. Our strategy was to cross mammary tumor-prone mice carrying the neu/erbB2 oncogene under control of the mouse mammary tumor virus (MMTV) promoter (20), with TSP1-null (5) and hTSP1-overexpressor lines of transgenic mice.

Materials and Methods

Generation of neu-*tbsp1*$^{-/-}$ and neu-hTSP1 Mice. TSP1-null mouse (*tbsp1*$^{-/-}$) has been reported (5). These animals were crossed into the FVB/N strain for the purpose of the present study (eight generations). Mice overexpressing human TSP1 (TgN-MMTV-hTSP1 FVB) were produced by microinjection of a linearized fragment of the MMTV-LTR-hTSP1 construct into one-cell FVB/N blastocysts. The generation, phenotype, and genotype of the resulting animals have been described elsewhere (M.A.O., J.C.R.-M., and M.L.I.-A., unpublished work). neu-transgenic animals (TgN-neu) were purchased from Charles River Breeding Laboratories. *tbsp1*$^{-/-}$ and TgN-MMTV-hTSP1 male mice were crossed successively with TgN-neu females to generate neu-*tbsp1*$^{-/-}$ and neu-hTSP1 mice, respectively.

Tumor Analysis. Tumor incidence was determined by daily examination of mammary glands for palpable tumors after animals reached 8 weeks of age. Curves depicting percentage of tumor-free mice as a function of time were assessed statistically and compared by using the log-rank test (21). Kinetic growth analysis was done every 5 days by caliper measurement with five animals per genotype, selected once tumors were palpable. For histological evaluation, mammary tumors were fixed in 4% paraformaldehyde by perfusion, dissected, and postfixed for 1–2 h at 4°C. Immunohistochemical analysis was performed by using the following antibodies: TSP1, a monoclonal antibody that recognized both human and

Abbreviations: ECM, extracellular matrix; MMP, matrix metalloproteinase; TSP, thrombospondin; VEGF, vascular endothelial growth factor; PECAM, platelet-endothelial adhesion molecule; MMTV, mouse mammary tumor virus.

¶To whom reprint requests should be addressed at: University of California, Boyer Hall, Room 559, 611 Charles E. Young Drive, Los Angeles, CA 90095. E-mail: arispe@mbi.ucla.edu.

The publication costs of this article were defrayed in part by page charge payment. This article must therefore be hereby marked "*advertisement*" in accordance with 18 U.S.C. §1734 solely to indicate this fact.

CELL BIOLOGY

mouse forms (22), platelet-endothelial adhesion molecule (PECAM) (BD PharMingen), VEGF (D. Senger), and GV39 M, which recognizes VEGF only when bound to VEGFR2 (a gift from P. Thorpe, Toshiba, Irvine, CA) (23).

Evaluation of vascular parameters was accomplished by analysis of PECAM-stained sections of five independent tumors (1 cm^3 from each genotype). Images were obtained randomly (two images from each tumor; 10 images total per phenotype) at ×10 on a Nikon Diaphot 300 microscope equipped with a Toshiba 3CCD camera. Number of vessels, vascular perimeter, and lumen area were obtained by using IMAGEPRO 4.0 software (Media Cybernetics, Silver Spring, MD). Assessment of tumor vasculature was also performed by i.v. injection of animals with FITC-conjugated *Lycopersicon esculentum* lectin (24).

In situ hybridization for mouse TSP1 mRNA was performed as described previously (25). Identification of human TSP1 transgene in mouse tissues was as described (22). Both probes had been tested for crossreactivity to other members of the TSP family, as mentioned in the cited references. Also, the human probe does not recognize the endogenous mouse transcripts.

ELISA Analysis. Levels of TSP1 were determined by a sandwich ELISA method. A monoclonal antibody that recognizes both mouse and human TSP1 (22) was bound to plates (50 μg/ml). After blocking, protein extracts were incubated overnight. Tissue extracts from *tbsp1*$^{-/-}$ mice showed negligible activity and provided a baseline for the assay. A second antibody made in rabbit (which also recognizes mouse and human TSP1) was used to detect total TSP1, followed by alkaline-phosphatase-conjugated anti-rabbit IgG. Levels of total TSP1 were determined in triplicate samples by comparison with a standard TSP1 curve present in each assay. The sensitivity was 10 pg. The intraassay coefficient of variation was 3.4%, and the interassay coefficient of variation averaged 7.6%.

Immunoblot Analysis and Zymography. Total protein from tumors and mammary glands was extracted in 10 mM Tris, pH 7.4/150 mM NaCl/1 mM $CaCl_2$/1 mM $MgCl_2$/0.1% Triton X-100, in the presence of the protease inhibitor mixture Complete (Roche Molecular Biochemicals). Protein content was determined by a colorimetric assay (Bio-Rad). In some cases, protein extracts were purified by affinity chromatography with heparin-Sepharose or gelatin-Sepharose beads (Amersham Pharmacia Biotech) and further concentrated with Centricon concentrators (Amicon).

Primary antibodies used were: human MMP9 (AB16996), mouse MMP9 (AB19047), and MMP2 (MAB13434), from Chemicon; and VEGF (a gift from D. Senger). Signal was detected by chemiluminescence (SuperSignal kit, Pierce, Rockford, IL).

Zymography was performed as described (26).

MMP9 Activation Assays *in Vitro*. Purified MMP9 (CC079, Chemicon) was preincubated for 2 h at 4°C in the presence or absence of TSP1 [purified from human platelets as described (27)], or different extracellular matrix (ECM) proteins as negative controls. Activation was performed in 15 mM Tris, pH 7.4/150 mM NaCl/1 mM $CaCl_2$, with MMP3 (CC1035, Chemicon), *p*-aminophenyl mercuric acetate (Sigma), or TPCK-treated trypsin (Sigma). ECM proteins used included: fibronectin (Sigma), collagen types I and VIII (a generous gift from Helene Sage, Heart Hope Institute, Seattle, WA).

Gelatinase Activity Assays. Dose-response analysis was performed by using the EnzChek Gelatinase Assay kit (Molecular Probes). Gelatinase activity was also detected by using the MMP gelatinase activity assay kit (Chemicon), which utilizes a biotinylated gelatinase substrate.

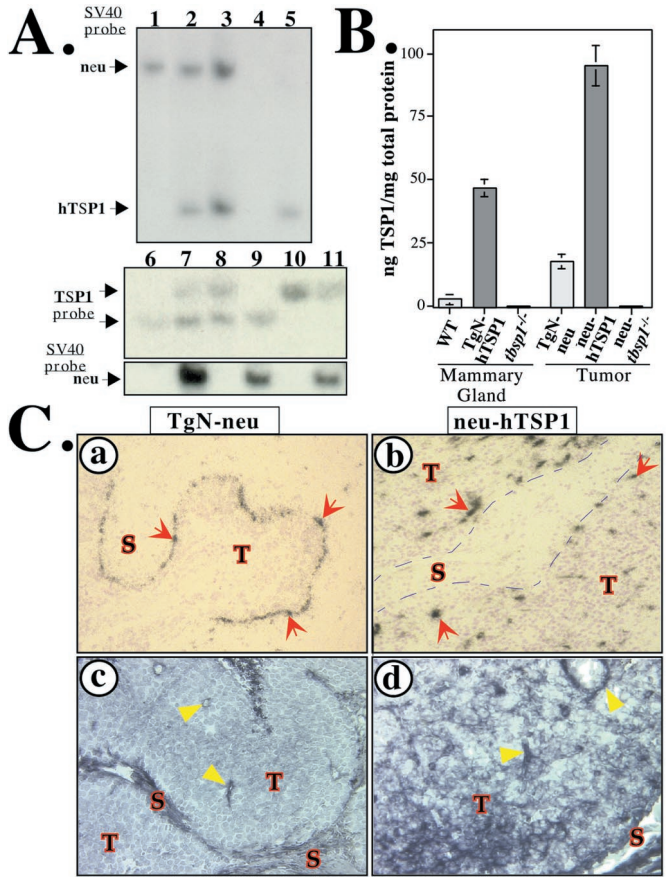

Fig. 1. Generation and analysis of transgenic animals. (*A*) Southern blots were probed with a fragment of the simian virus 40 polyA sequence that identifies a 7.5-kb band for the neu (lanes 1, 2, 3, 7, 9, and 11) and a 0.9-kb band for the human TSP1 transgenes (lanes 2, 3, and 5), respectively. A mouse TSP1 probe was used to identify offspring homozygous for the mutated allele (*tbsp1*$^{-/-}$) (5.8 kb) (lanes 10 and 11), homozygous for the wild-type allele (4.4 kb) (lanes 6 and 9), or heterozygous with both alleles (lanes 7 and 8). (*B*) ELISA analysis of total TSP1 protein levels from: (*i*) wild type (WT), TgN-hTSP1 and *tbsp1*$^{-/-}$ mammary gland tissue; and (*ii*) TgN-neu, neu-hTSP1, and neu-*tbsp1*$^{-/-}$ mammary tumor tissue. Bars indicate standard error. (*C*) Localization of TSP1 in tumors. *In situ* hybridization for mouse TSP1 mRNA in TgN-neu (a) and for human TSP1 mRNA in neu-hTSP1 (b) tumors. Immunodetection of TSP1 protein on TgN-neu (c) and neu-hTSP1 (d) tumors. Red arrows indicate TSP1 expression and dashed line (in b) denotes the boundary between tumor and stroma. Yellow arrowheads identify blood vessels. T, tumor; S, Stroma.

Results

Generation of Mice and Tumor Analysis. Tumor formation was induced by overexpression of activated neu oncogene under the control of MMTV promoter. These animals (TgN-neu) reproducibly develop mammary adenocarcinomas that arise spontaneously between 12 and 20 weeks of age, as foci in hyperplastic and dysplastic epithelia (20). Depletion of TSP1 was achieved by crossing TgN-neu mice with animals deficient in TSP1 (*tbsp1*$^{-/-}$) (5); such animals are identified as neu-*tbsp1*$^{-/-}$ in the text. A third group was generated by crossing the TgN-neu mice with a transgenic line that overexpressed the human TSP1 protein (TgN-hTSP1), also under the control of MMTV promoter/enhancer elements (M.A.O., J.C.R.-M., and M.L.I.-A., unpublished work); these animals are identified in the text as neu-hTSP1. All mice shared the same genetic background (FVB/N) to eliminate contributions from modifier loci.

Genotyping was performed by Southern blot (Fig. 1*A*) and PCR analysis. The expression of TSP1, both mouse (endoge-

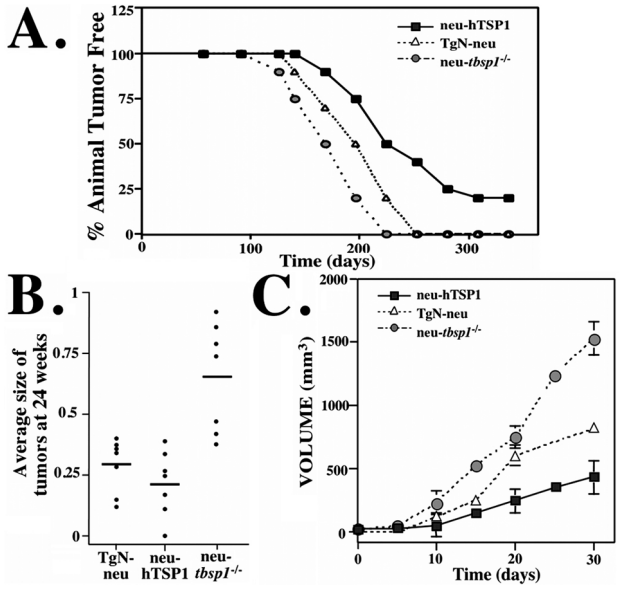

Fig. 2. Characterization of tumors. (*A*) Tumor formation in transgenic female carriers of neu alone (TgN-neu) or neu in the absence (neu-*tbsp1*$^{-/-}$) or presence of constitutive TSP1 (neu-hTSP1) were followed for 48 weeks. The trend for earlier appearance of tumors across the three groups was statistically significant ($P < 0.001$). Pair-wise comparisons demonstrated that the differences among the three curves were also statistically significant ($P < 0.01$). $n = 20$ in each category. (*B*) Average size of tumors at 24 weeks. The difference between neu-*tbsp1*$^{-/-}$ and TgN-neu tumors was statistically significant ($P = 0.0039$, Student's *t* test). (*C*) Kinetics of tumor growth over 30 days. Average values ± SE are presented ($n = 5$).

nous) and human (transgene), in mammary glands was confirmed by Northern blot analysis (data not shown). Twenty-two TgN-neu, 34 neu-*tbsp1*$^{-/-}$, and 27 neu-hTSP1 animals were used in this study. We observed that tumors arose independently and asynchronously in all three groups of mice. In most cases, more than one mammary gland was affected with several tumors (TgN-neu, $\chi = 2.42 \pm 1.2$; neu-*tbsp1*$^{-/-}$, $\chi = 5.85 \pm 2.8$; neu-hTSP1, $\chi = 1.85 \pm 1.8$). Animals were killed when any one tumor reached 1.5 cm in diameter, or after 18 months.

Mammary glands from wild-type animals showed low but detectable levels of TSP1 protein (Fig. 1*B*). A near 18-fold increase was found in transgenic glands from TSP1-overexpressing animals in the absence of adenocarcinomas. Tumors from TgN-neu animals showed a 4-fold increase in TSP1 levels over nonpathological states of the tissue (mammary gland of wild-type group). A 5.5-fold increase in TSP1 protein was detected in tumors from TgN-hTSP1 versus tumors from TgN-neu group. TSP1 mRNA was localized in the reactive stroma that limits the evolving tumor (Fig. 1*C*a) in TgN-neu mice. This pattern of expression differs from the one displayed by neu-hTSP1 mice, where strong signal for hTSP1 mRNA was found in tumor cells (Fig. 1*C*b). Immunohistological analysis was consistent with these findings (Fig. 1*C* c and d).

A detailed analysis of tumor progression in the three study groups revealed variations in time of tumor onset and kinetics of tumor growth (Fig. 2). Mammary tumors first appeared at 91, 126, and 168 days in neu-*tbsp1*$^{-/-}$, TgN-neu, and neu-TSP1 animals, respectively. The median age for tumor onset was also different when neu-*tbsp1*$^{-/-}$ and neu-hTSP1 groups were compared (168 days vs. 224, respectively) (Fig. 2*A*). Even more significantly, all neu-*tbsp1*$^{-/-}$ animals developed tumors by 224 days, whereas 20% of neu-hTSP1 remained tumor free for the duration of the study (18 months). This last set of animals did develop areas of parenchymal hyperplasia, as detected by carmine staining of the glands at the end of the study (data not shown). However, these hyperplastic nodules failed to evolve into frank tumors. Furthermore, the average size of tumors (Fig. 2*B*) and kinetics of growth (Fig. 2*C*) were accelerated in the absence of TSP1.

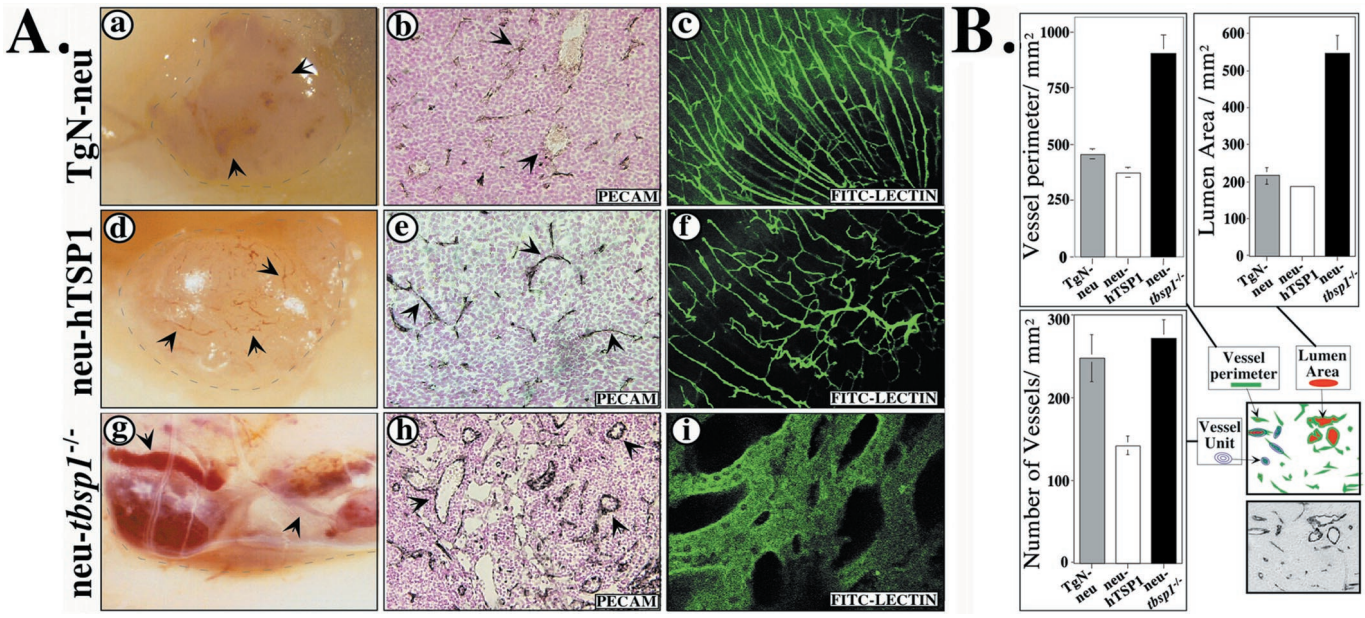

Fig. 3. Vascular profile of tumors. (*A*) Evaluation of TgN-neu (a–c), neu-hTSP1 (d–f), and neu-*tbsp1*$^{-/-}$ (g–i) tumors. a, d, and g, show macroscopic images of tumors. In b, e, and h, vessels are identified with a PECAM antibody. In c, f, and i, vascular structures are visualized after a single intravascular injection of FITC-conjugated lectin followed by confocal microscopy. (*B*) Quantitation of vascular parameters. Real and computerized images of vessel perimeter (green), lumen area (red), and vessel number are shown alongside quantitation. Bars indicate standard error. Statistical significance (Student's *t* test) was found between neu-*tbsp1*$^{-/-}$ and TgN-neu groups for vessel perimeter ($P = 0.001$) and for lumen area ($P = 0.00046$). For number of vessels, statistical significance (Student's *t* test) was found between TgN-neu and neu-hTSP1 tumors ($P = 0.006$).

Histological evaluation of tumors from all genotypes revealed very similar poorly differentiated adenocarcinomas. In contrast, marked differences in vascularization of the tumors were evident even macroscopically (Fig. 3*A*, first column). Tumors from neu-*tbsp1*$^{-/-}$ mice showed a red surface with visible large vessels, in contrast to the whitish color and paucity of major vessels on the surface of neu-hTSP1 tumors. Microscopic evaluation showed that vessels in animals that lack TSP1 were dilated, whereas capillaries from neu-hTSP1 tumors were discrete and less frequent (Fig. 3*A*, second column). Visualization of vessels with FITC-conjugated lectin provided further evidence of complex changes in the entire vascular architecture (Fig. 3*A*, third column). Quantification of the vascular parameters in tumors better reflected these aberrations (Fig. 3*B*). Vessel perimeter was determined as total positive staining area with a PECAM antibody. neu-*tbsp1*$^{-/-}$ tumors showed a significant 2-fold increase in vessel perimeter when compared with TgN-neu. In contrast, this parameter in neu-hTSP1 tumors was reduced (1.2-fold) compared with the TgN-neu group control. Quantification of the lumen area was also evaluated as a measure of vascular dilation. These data showed a significant 2.6-fold increase in neu-*tbsp1*$^{-/-}$ when compared with neu-hTSP1 tumors. Changes in vascular lumen were not an artifactual result of fixation, because these parameters were assessed in tumors fixed by perfusion. Finally, we determined vessel density as number of vascular profiles per mm^2. Interestingly, a significant reduction of vessel number was found in tumors with overexpression of hTSP1, but no significant increase was noted in neu-*tbsp1*$^{-/-}$ tumors versus TgN-neu group control (Fig. 3*B*).

Together, these results strongly support the conclusion that TSP1 is a negative regulator of tumor vasculature, and that vascularization correlates with both tumor growth kinetics and time of incidence. In addition, our data provide evidence of a role for TSP1 in regulating vessel morphology.

Gelatinase Activity in Tumors. To ascertain the molecular basis for the alteration in vascular morphology, we assessed the levels of several ECM proteins and proteases. Our analysis included quantitative analysis of several collagens (types I, III–V), glycoproteins (fibronectin, laminin, nidogen), and proteases [gelatinases A (MMP2) and B (MMP9), urokinase-plasminogen activator, and tissue-plasminogen activator)]. Significant and consistent changes were seen only for MMP9. Gelatin zymography was used to identify both zymogen and active forms (28) (Fig. 4*A*). Although proMMP9 was found in all of the tumors, active MMP9 was detected at different proportions in tumors derived from each of the three genotypes. Active MMP9 was clearly reduced in neu-hTSP1 tumors and was increased in neu-*tbsp1*$^{-/-}$. Densitometric quantification of pro- and active MMP9 forms revealed significant differences in the percentage of active MMP9 present in tumors of each genotype (Fig. 4*A*). The activation status of MMP9 was confirmed by immunoblot analysis (Fig. 4*B*). When compared with wild-type mammary gland, we observed that MMP9 was increased in all tumors, whereas MMP2 was present at low levels (data not shown) and did not change on the tumors in relation to TSP1 expression (Fig. 4*C*).

Increased levels of active MMP9 could explain the more invasive phenotype, rapid growth, and greater vascularity displayed by the neu-*tbsp1*$^{-/-}$ tumors. These results would also suggest a role of TSP1 as an inhibitor of MMP9 activation. High levels of hTSP1 in the neu-hTSP1 animals were associated with decreased active MMP9, although overall levels of proMMP9 were similar. In the absence of TSP1 in the neu-*tbsp1*$^{-/-}$ animals, the converse was observed and resulted in an unusual increase of active MMP9.

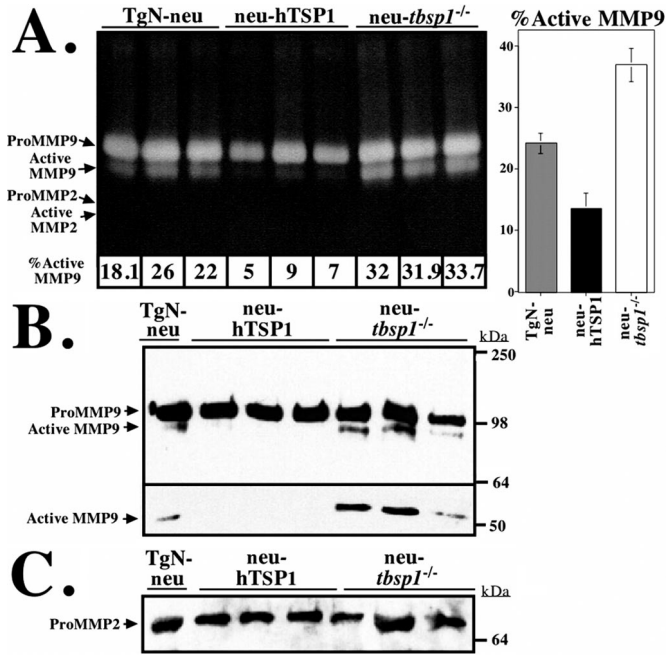

Fig. 4. Expression of gelatinases in tumors. (*A*) Gelatin zymography of tumor extracts (5 μg of protein). Percentage of active versus total MMP9 is shown for each lane. The graph represents a summary of the percentage of active MMP9 versus total MMP9 for each group. Differences are statistically significant (Student's *t* test) compared with TgN-neu control group (for neu-hTSP1, $P = 0.01$; and for neu-*tbsp1*$^{-/-}$, $P = 0.002$). (*B*) Immunoblot analysis of tumor extracts with MMP9 antibody. Two images of the blot appear representing different exposure times to show the rarer low-molecular-weight active MMP9 form. (*C*) The same blot was reprobed with MMP2 antibody.

MMP9 Activation Is Inhibited by TSP1. To better evaluate the participation of TSP1 in the regulation of MMP9 processing, we tested the effects of purified TSP1 on proMMP9 activation by MMP3. MMP3 (also known as stromelysin-1) is the most efficient activator of MMP9 identified to date, and it has been proposed as a likely candidate for a physiological activator of MMP9 *in vivo* (29). Activation of the 92-kDa proMMP9 zymogen to the 82- and 67-kDa active forms was inhibited in the presence of TSP1 (Fig. 5*A*). The processing/activation of MMP9 was confirmed by both immunoblot and zymography analysis. In the presence of the organic compound *p*-aminophenyl mercuric acetate, a nonspecific activator of matrix metalloproteinases, TSP1 did not affect activation (Fig. 5*A*).

To assess the functional relevance of TSP1 inhibition of MMP9 processing, we evaluated the effect of TSP1 on MMP9 activity. Activation of proMMP9 by MMP3 was performed in the absence or presence of TSP1 and analyzed by zymography to estimate the activation status (Fig. 5*B Inset*). These same samples were also assayed for gelatinase activity. To distinguish between the effect of TSP1 on processing versus a potential inhibition of MMP9 activity, TSP1 was added to already active MMP9 (Fig. 5*B*, lane 4). TSP1 had no inhibitory effect on active MMP9. Inhibition of gelatinase activity was significant only when TSP1 was present during the activation process (Student's *t* test, $P = 0.000014$). These results suggested that the effect of TSP1 occurs by blocking processing/activation of proMMP9. In contrast to the effect of tissue inhibitors of matrix metalloproteases (30, 31), TSP1 does not directly affect enzymatic activity of the protease once it has been processed. Finally, the inhibitory effect of TSP1 on MMP9 activation by MMP3 was shown to occur in a dose-dependent manner (Fig. 5*C*).

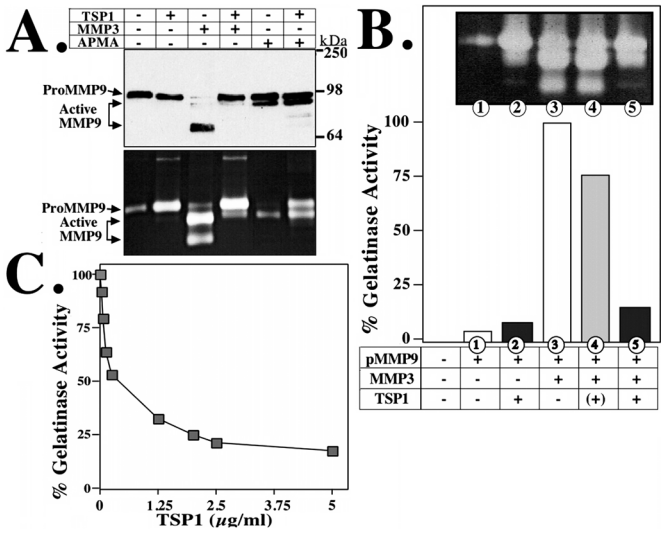

Fig. 5. *In vitro* inhibition of MMP9 activation by TSP1. (*A*) Purified proMMP9 preincubated in the presence or absence of purified TSP1 was subsequently treated with the activators MMP3 or *p*-aminophenyl mercuric acetate. The reaction was analyzed by immunoblot (*Top*) and gelatin zymography (*Bottom*). (*B*) Purified proMMP9 preincubated in the absence (1, 3, and 4) or presence of TSP1 (2 and 5) was left untreated (1 and 2) or treated with MMP3 (3–5). After MMP3 activation, TSP1 was added to sample 4. All samples were analyzed for gelatinase activity. Data are presented as percentage of maximum activation with MMP3. Each reaction was also analyzed by zymography (*Inset*). (*C*) Purified proMMP9 preincubated in the presence of increasing amounts of TSP1 was treated with MMP3. Half of the reaction was diluted in 200 μl and analyzed for gelatinase activity. Data are presented as percentage of maximum activation with MMP3. Each point represents the average of three independent experiments.

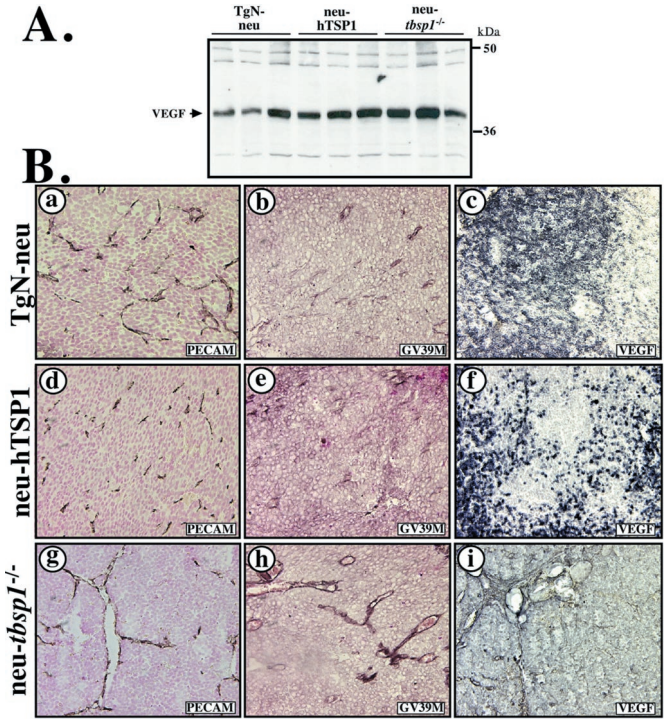

Fig. 6. Evaluation of VEGF levels and distribution in tumors. (*A*) Equal protein amounts were analyzed by immunoblot with a specific antibody for VEGF. (*B*) Mammary tumor sections from TgN-neu (a–c), neu-hTSP1 (d–f), neu-*tbsp1*$^{-/-}$ (g–i) mice were evaluated for expression of VEGF by using two antibodies: GV39 M, which recognizes VEGF bound to VEGFR2 (b, e, h) and a polyclonal anti-mouse VEGF, which recognizes the receptor-free form (c, f, i). Staining with PECAM-specific antisera was used for identification of vessels (a, d, g).

Distribution of VEGF. MMP2 and MMP9 play critical roles in matrix degradation and have been shown to modulate neovascularization. In addition, release of growth factors from the ECM has been attributed to matrix metalloproteinases (32–34). In particular, MMP9 has been shown to release VEGF from extracellular stores (35). VEGF is a vascular morphogen whose modulation could explain some of the vascular alterations observed in our tumor model. The tortuous, dilated, and abundant vascular networks characteristic of the neu-*tbsp1*$^{-/-}$ tumors are, in fact, reminiscent of phenotypes attributed to elevated VEGF (36–38).

Although levels of VEGF mRNA (data not shown) and protein (Fig. 6*A*) from tumors of all genotypes were not significantly different, immunohistochemical analysis demonstrated changes in the distribution of this growth factor. The use of specific antibodies that recognize VEGF bound to VEGFR2 (GV39 M) (23) or receptor-free VEGF revealed that, in neu-*tbsp1*$^{-/-}$ tumors, abundant VEGF protein was complexed to VEGFR2 (Fig. 6*B*h); in contrast, this association was not as evident in the neu-hTSP1 tumors (Fig. 6*B*e). Receptor-free VEGF appeared largely associated with the surface of tumor cells and bound to ECM components (Fig. 6*B* c, f, and i).

Discussion

In the present study, we evaluated the contribution of TSP1 to spontaneous tumor progression in breast cancer-prone mice. All of the animals used were inbred on the FVB/N background, and therefore the study was controlled with respect to potential modifier loci. This model served to address two issues important in tumor development: (*i*) the relative contribution of endogenous angiogenic inhibitors to tumor onset and growth, and (*ii*) the mechanism by which TSP1 regulates neovascular recruitment in breast carcinomas.

The hypothesis that TSP1 functions as a suppressor of capillary growth is now over 10 years old (4). Much research has been performed to determine specific regions of the molecule responsible for its antiangiogenic activity (10, 27). The mechanism of action of TSP1 has been shown to include activation of CD36, p59Fyn, and caspase resulting in apoptosis, as well as activation of transforming growth factor β (11, 39). Our results include direct regulation of MMP9 activation as an additional mechanism. It is likely that a combination of all these effects contributes to TSP1-mediated suppression of tumor angiogenesis.

Cleavage of ECM components is a key requirement for migration of cells, and proteolysis allows release of growth factors and other signaling molecules from extracellular stores. More than a decade ago, Vlodavsky and colleagues showed that heparitinase was able to release fibroblast growth factor 2 from the subendothelial ECM, introducing the concept that growth factor availability could be controlled by selective release from the extracellular environment (40). Subsequent reports have shown that proteases can perform similar functions. A direct role for MMP9 in the regulation of angiogenesis via modulation of growth factor availability was initially demonstrated in homozygous mice with a null mutation in MMP9 (33). More recently, it has been clearly demonstrated that MMP9 mediates release of VEGF from extracellular stores, and that this protease mediates the angiogenic switch (35). In our model, we found a significant difference in the levels of active MMP9 in TSP1-null animals. Higher levels of active MMP9 could potentially facilitate tumor expansion and angiogenesis by release of endothelial growth factors from the matrix. Additional experiments demonstrated that TSP1 suppresses activation of MMP9 by both MMP3 and trypsin. This activity could partially account for the suppressive

effects of TSP1 on endothelial cell migration. Also, inhibition of growth factor availability to endothelial cells could contribute to the apoptotic effects of TSP1 on endothelial cells *in vivo*.

Recently, the use of antibodies generated against an epitope that recognized VEGF bound to VEGFR2 has demonstrated that the level of "bioactive" VEGF is relatively low and is specifically bound to vessels that are in the process of angiogenic remodeling (23). The concept that TSP1 could contribute to the regulated release of VEGF from extracellular stores is an attractive one. By using specific antibodies against VEGF and against VEGF/VEGFR2 complex (23), we have found differences in the distribution of VEGF that correlate with TSP1 production. An increase in "bioactive" VEGF could contribute to the increase in vascular density and the enlarged vascular morphology displayed by the TSP1-deficient tumors. Additional experiments, however, are required to verify this model.

The participation of TSP1 as modulator of enzymatic activity has been previously acknowledged. Specifically, TSP1 has been shown to bind to and inhibit plasmin, neutrophil elastase, and cathepsin G activities (41). Tuszynski and colleagues had previously reported that addition of TSP1 to endothelial cultures increase MMP9 levels (42). We found, as these authors, that exogenous TSP1 added to microvascular endothelial cultures leads to accumulation and stabilization of proMMP9, as can be detected by zymography. However, this increase occurs with a parallel reduction in MMP9 activation/processing (J.C.R.-M. and M.L.I.-A., unpublished observations). More recently, the type I repeats of TSP1 and TSP2 were shown to bind to MMP2 in a yeast two-hybrid screen, and binding was further confirmed with both MMP2 and MMP9 *in vitro* by coimmunoprecipitation by using purified proteins (43). The authors also demonstrated that presence of TSP1 blocks gelatinolytic activity of these enzymes and speculated that the effect of TSPs might be mediated via block of proMMP2 and proMMP9 processing. Our data are in agreement with these observations and further demonstrate that regulation of MMP9 processing is a relevant function of TSP1 in tumor settings. Furthermore, TSP2 has been shown to regulate MMP2 availability via the low-density lipoprotein-related receptor protein receptor (44). Together these findings are consistent with a role of TSP1 and -2 in the regulation of MMP activity and are in concert with the reported effects of TSP1 as an inhibitor of migration, invasion and angiogenesis.

We thank Drs. Don Senger (Beth Israel Medical Deaconess Center, Boston, MA) and Phil Thorpe and Rolf Brekken (University of Texas Southwestern Medical Center, Dallas, TX) for generous provision of antibodies, Dr. Elliot Landaw (BASE Unit at University of California, Los Angeles) for statistical support, Sarah Oikemus for excellent technical assistance, and members of M.L.I.-A.'s lab for helpful discussion. This work was supported by grants from the Department of Defense Army (DAMD 17–94-J-4346), the National Cancer Institute [R29CA65624-05 and the R01CA77420 (to M.L.I.-A.) and CA16042 (to E.L.)], and the National Heart, Lung, and Blood Institute (HL28749 to J.L.).

1. Hanahan, D. & Weinberg, R. A. (2000) *Cell* **100,** 57–70.
2. Hanahan, D. & Folkman, J. (1996) *Cell* **86,** 353–364.
3. Kerbel, R. S. (2000) *Carcinogenesis* **21,** 505–515.
4. Good, D. J., Polverini, P. J., Rastinejad, F., Le Beau, M. M., Lemons, R. S., Frazier, W. A. & Bouck, N. P. (1990) *Proc. Natl. Acad. Sci. USA* **87,** 6624–6628.
5. Lawler, J., Sunday, M., Thibert, V., Duquette, M., George, E. L., Rayburn, H. & Hynes, R. O. (1998) *J. Clin. Invest.* **101,** 982–992.
6. Brown, L. F., Guidi, A. J., Schnitt, S. J., Van De Water, L., Iruela-Arispe, M. L., Yeo, T. K., Tognazzi, K. & Dvorak, H. F. (1999) *Clin. Cancer Res.* **5,** 1041–1056.
7. Reed, M. J., Iruela-Arispe, L., O'Brien, E. R., Truong, T., LaBell, T., Bornstein, P. & Sage, E. H. (1995) *Am. J. Pathol.* **147,** 1068–1080.
8. Polverini, P. J., DiPietro, L. A., Dixit, V. M., Hynes, R. O. & Lawler, J. (1995) *FASEB J.* **9,** A272.
9. Vogel, T., Guo, N., Krutzsch, H. C., Blake, D. A., Hartman, J., Mendelovitz, S., Panet, A. & Roberts, D. D. (1993) *J. Cell. Biochem.* **53,** 74–84.
10. Tolsma, S. S., Volpert, O. P., Good, D. J., Frazier, W. A., Polverini, P. J. & Bouck, N. (1993) *J. Cell Biol.* **122,** 497–511.
11. Jimenez, B., Volpert, O. V., Crawford, S. E., Febbrario, M., Silverstein, R. L. & Bouck, N. (2000) *Nat. Med.* **6,** 41–48.
12. Guo, N. H., Krutzsch, H. C., Inman, J. K. & Roberts, D. D. (1997) *Cancer Res.* **57,** 1735–1742.
13. Volpert, O. V., Lawler, J. & Bouck, N. P. (1998) *Proc. Natl. Acad. Sci. USA* **95,** 6343–6348.
14. Sheibani, N. & Frazier, W. A. (1995) *Proc. Natl. Acad. Sci. USA* **92,** 6788–6792.
15. Bleuel, K., Popp, S., Fusenig, N. E., Stanbridge, E. J. & Boukamp, P. (1999) *Proc. Natl. Acad. Sci. USA* **96,** 2065–2070.
16. Streit, M., Velasco, P., Brown, L. F., Skobe, M., Richard, L., Riccardi, L., Lawler, J. & Detmar, M. (1999) *Am. J. Pathol.* **155,** 441–452.
17. Guo, N. H., Krutzsch, H. C., Inman, J. K., Shannon, C. S. & Roberts, D. D. (1997) *J. Pept. Res.* **50,** 210–221.
18. Zabrenetzky, V., Harris, C. C., Steeg, P. S. & Roberts, D. D. (1994) *Int. J. Cancer* **59,** 191–195.
19. Weinstat-Saslow, D. L., Zabrenetzky, V. S., VanHoutte, K., Frazier, W. A., Roberts, D. D. & Steeg, P. S. (1994) *Cancer Res.* **54,** 6504–6511.
20. Muller, W. J., Sinn, E., Pattengale, P. K., Wallace, R. & Leder, P. (1988) *Cell* **54,** 105–115.
21. Altman, D. G. (1991) *Practical Statistics for Medical Research* (Chapman & Hall/CRC, Boca Raton, FL).
22. Iruela-Arispe, M. L., Porter, P., Bornstein, P. & Sage, E. H. (1996) *J. Clin. Invest.* **97,** 403–412.
23. Brekken, R. A., Huang, X., King, W. W. & Thorpe, P. E. (1998) *Cancer Res.* **58,** 1952–1959.
24. Murphy, T. J., Thurston, G., Ezaki, T. & McDonald, D. M. (1999) *Am. J. Pathol.* **155,** 93–103.
25. Iruela-Arispe, M. L., Liska, D. J., Sage, E. H. & Bornstein, P. (1993) *Dev. Dyn.* **197,** 40–56.
26. Rodríguez-Manzaneque, J. C., Graubert, M. & Iruela-Arispe, M. L. (2000) *Hum. Reprod.* **15,** 39–47.
27. Iruela-Arispe, M. L., Lombardo, M., Krutzsch, H. C., Lawler, J. & Roberts, D. D. (1999) *Circulation* **100,** 1423–1431.
28. Talhouk, R. S., Chin, J. R., Unemori, E. N., Werb, Z. & Bissell, M. J. (1991) *Development (Cambridge, U.K.)* **112,** 439–449.
29. Ramos-DeSimone, N., Hahn-Dantona, E., Sipley, J., Nagase, H., French, D. L. & Quigley, J. P. (1999) *J. Biol. Chem.* **274,** 13066–13076.
30. Ogata, Y., Itoh, Y. & Nagase, H. (1995) *J. Biol. Chem.* **270,** 18506–18511.
31. Olson, M. W., Bernardo, M. M., Pietilla, M., Gervasi, D. C., Toth, M., Kotra, L. P., Massova, I., Mobashery, S. & Fridman, R. (2000) *J. Biol. Chem.* **275,** 2661–2668.
32. Naldini, L., Vigna, E., Bardelli, A., Follenzi, A., Galimi, F. & Comoglio, P. M. (1995) *J. Biol. Chem.* **270,** 603–611.
33. Vu, T. H., Shipley, J. M., Bergers, G., Berger, J. E., Helms, J. A., Hanahan, D., Shapiro, S. D., Senior, R. M. & Werb, Z. (1998) *Cell* **93,** 411–422.
34. Whitelock, J. M., Murdoch, A. D., Iozzo, R. V. & Underwood, P. A. (1996) *J. Biol. Chem.* **271,** 10079–10086.
35. Bergers, G., Brekken, R., McMahon, G., Vu, T. H., Itoh, T., Tamaki, K., Tanzawa, K., Thorpe, P., Itohara, S., Werb, Z. & Hanahan, D. (2000) *Nat. Cell Biol.* **2,** 737–744.
36. Thurston, G., Suri, C., Smith, K., McClain, J., Sato, T. N., Yancopoulos, G. D. & McDonald, D. M. (1999) *Science* **286,** 2511–2514.
37. Pettersson, A., Nagy, J. A., Brown, L. F., Sundberg, C., Morgan, E., Jungles, S., Carter, R., Krieger, J. E., Manseau, E. J., Harvey, V. S., *et al.* (2000) *Lab. Invest.* **80,** 99–115.
38. Detmar, M., Velasco, P., Richard, L., Claffey, K. P., Streit, M., Riccardi, L., Skobe, M. & Brown, L. F. (2000) *Am. J. Pathol.* **156,** 159–167.
39. Crawford, S. E., Stellmach, V., Murphy-Ullrich, J. E., Ribeiro, S. M. F., Lawler, J., Hynes, R. O., Boivin, G. P. & Bouck, N. (1998) *Cell* **93,** 1159–1170.
40. Bashkin, P., Doctrow, S., Klagsbrun, M., Svahn, C. M., Folkman, J. & Vlodavsky, I. (1989) *Biochemistry* **28,** 1737–1743.
41. Hogg, P. J. (1994) *Thromb. Haemost.* **72,** 787–792.
42. Qian, X., Wang, T. N., Rothman, V. L., Nicosia, R. F. & Tuszynski, G. P. (1997) *Exp. Cell. Res.* **235,** 403–412.
43. Bein, K. & Simons, M. (2000) *J. Biol. Chem.* **275,** 32167–32173.
44. Yang, Z., Strickland, D. K. & Bornstein, P. (2001) *J. Biol. Chem.* **276,** 8403–8408.